NANO LETTERS

Letter

pubs.acs.org/NanoLett

Redox Sorting of Carbon Nanotubes

Hui Gui,[†] Jason K. Streit,[§] Jeffrey A. Fagan,[§] Angela R. Hight Walker,[∥] Chongwu Zhou,*[,‡] and Ming Zheng*[,§]

[†]Department of Chemical Engineering and Materials Science and [‡]Department of Electrical Engineering, University of Southern California, Los Angeles, California 90089, United States

[§]Materials Science and Engineering Division and [∥]Semiconductor and Dimensional Metrology Division, National Institute of Standards and Technology, 100 Bureau Drive, Gaithersburg, Maryland 20899, United States

Supporting Information

ABSTRACT: This work expands the redox chemistry of single-wall carbon nanotubes (SWCNTs) by investigating its role in a number of SWCNT sorting processes. Using a polyethylene glycol (PEG)/dextran (DX) aqueous two-phase system, we show that electron-transfer between redox molecules and SWCNTs triggers reorganization of the surfactant coating layer, leading to strong modulation of nanotube partition in the two phases. While the DX phase is thermodynamically more favored by an oxidized SWCNT mixture, the mildly reducing PEG phase is able to recover SWCNTs from oxidation and extract them successively from the DX phase. Remarkably, the extraction order follows SWCNT bandgap: semiconducting nanotubes of larger bandgap first, followed by semiconducting nanotubes of smaller bandgap, then nonarmchair metallic tubes of small but nonvanishing bandgap, and finally armchair metallic nanotubes of zero bandgap. Furthermore, we show that redox-induced surfactant reorganization is a common phenomenon, affecting nanotube buoyancy in a density gradient field, affinity to polymer matrices, and solubility in organic solvents. These findings establish redox modulation of surfactant coating structures as a general mechanism for tuning a diverse range of SWCNT sorting processes and demonstrate for the first time that armchair and nonarmchair metallic SWCNTs can be separated by their differential response to redox.

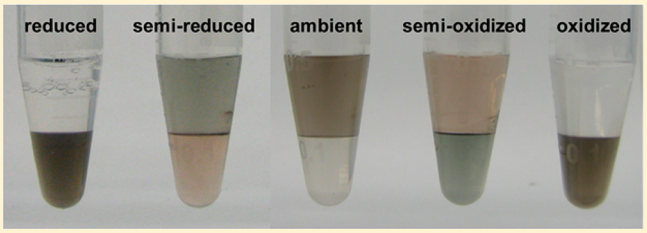

KEYWORDS: *Redox, carbon nanotube separation, surfactant coating structure, aqueous two-phase extraction*

The discovery of single-wall carbon nanotubes (SWCNTs) has unveiled the existence of not just one but a family of several hundred stable macromolecules.[1] They are all made of carbon atoms locally bonded in the hexagon geometry of graphene, but variations in the helical twist angle (θ) of the hexagons and in tube diameter (d) result in a diverse set of nanotube electronic structures. On the basis of theoretical analysis[2−5] and experimental observation,[6,7] all SWCNTs can be ranked in an order according to the width of their electronic bandgap: armchair metallic tubes ($\theta = 30°$) with zero bandgap; nonarmchair semimetallic tubes with small (<100 meV) but nonvanishing bandgaps that scale as $\cos(3\theta)/d^2$; and semiconducting tubes with bandgaps that scale as $1/d$.

The bandgap-based nanotube ranking manifests itself in solution phase SWCNT redox chemistry, a research subject started over a decade ago with the emergence of effective nanotube dispersion and separation methods. Strano et al. first observed that dissolved oxygen at low pH suppresses SWCNT optical absorption and resonance Raman cross sections in a bandgap-dependent fashion: metallic tubes are more sensitive than semiconducting tubes, and among the latter, the smaller bandgap/larger diameter tubes are more sensitive than larger bandgap/smaller diameter tubes.[8] Shortly after, Zheng and Diner showed that outer sphere electron transfer between SWCNTs and small-molecule oxidants also exhibits the same bandgap dependence and interpreted the oxygen- and pH-dependent optical response as the result of an outer-sphere electron transfer redox reaction between SWCNTs and oxygen.[9] Many ensuing studies have aimed at determining the redox potential of SWCNTs and its correlation with bandgap.[10,11]To further explore SWCNT redox chemistry, we find it useful to take a note from the classical coordination chemistry of transition metal ions, where ligand modulation of redox potential and ligand reorganization upon electron transfer are abundantly documented. If we view a dispersed SWCNT as a coordination complex, coupling is expected between the nanotube and the coordinating surfactant layer in electron transfer reactions.

In this work, we expand the redox chemistry of SWCNTs by investigating the effect of electron transfer on surfactant coating structures in the context of a number of SWCNT separation processes. Scheme 1 summarizes the basic chemistry at the focal point of this study. In the scheme, a black circle represents an individual nanotube, while the red and blue lines denote the

Received: October 31, 2014
Revised: February 14, 2015
Published: February 26, 2015

DOI: 10.1021/nl504189p
Nano Lett. 2015, 15, 1642−1646

Scheme 1

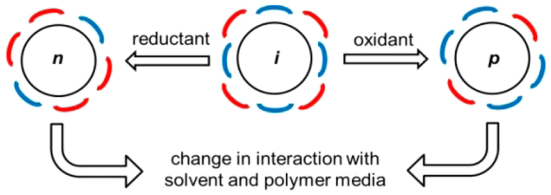

surfactant coating layer. Our findings suggest that electron transfer between SWCNTs and exogenous redox molecules induces surfactant coating layer reorganization, which in turn changes the interaction between dispersed SWCNTs and their solvent media, therefore altering the outcome of a number of separation processes. In keeping with solid state physics nomenclature, we denote the oxidized, resting, and reduced state by p, i, and n, respectively.

We first observed a strong redox effect in the separation of SWCNTs by the recently developed polymer aqueous two-phase (ATP) method.[12−14] Figure 1 shows the redox

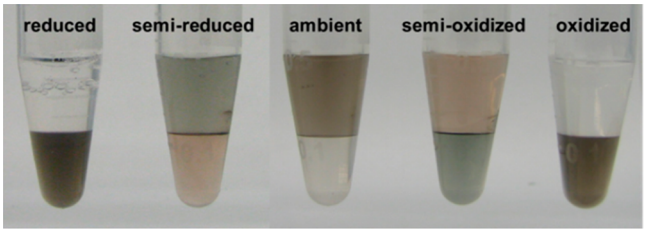

Figure 1. Redox modulation of nanotube partition in a 6% PEG + 6% DX two-phase system. The same amount of arc-discharge SWCNTs (Hanwha) and an identical surfactant composition 0.9% SC + 0.4% SDS are used in all cases. Redox agent added in each case: 200 mM $NaBH_4$ for the "reduced" regime; 70 mM $NaBH_4$ for the "semi-reduced" regime, nothing for the "ambient" regime; 0.5 mM NaClO for the "semi-oxidized" regime; and 2 mM NaClO for the "oxidized" regime.

modulation of SWCNT partition in a polyethylene glycol (PEG)/dextran (DX) system (see Supporting Information for experimental details). Arc-discharge SWCNTs were used in this particular experiment, but similar results were also observed for nanotubes with other diameter ranges. As shown in Figure 1, five distinct partition regimes can be created under different redox conditions: (1) a "reduced" regime, where both metallic and semiconducting tubes are found in the DX phase; (2) a "semi-reduced" regime, where metallic and semiconducting tubes are found in PEG and DX phase, respectively (see Supporting Information Figure S1 for the optical absorption spectra); (3) an "ambient" regime, where both metallic and semiconducting tubes are found in the top PEG phase; (4) a "semi-oxidized" regime, where metallic and semiconducting tubes are found in DX and PEG phase, respectively (see Supporting Information Figure S1 for the optical absorption spectra), reversing the partition found in the "semi-reduced" regime; (5) an "oxidized" regime, where both semiconducting and metallic tubes are pushed to the bottom DX phase.

While both oxidants and reductants can generate partition conditions for SWCNT sorting, we find that the oxidative process gives a broader tuning range for partition control. This is due in part to a built-in oxidant gradient across the two polymer phases. It has been reported that PEG has mild reducing capability.[15] Consistent with this, by monitoring changes in SWCNT optical absorbance induced by oxidation, we find that ∼ mM NaClO are consumed in 6% PEG solution within 1 min. In contrast, NaClO is quite stable in DX and capable of oxidizing nanotubes. When NaClO is added to a PEG/DX ATP system, PEG cannot effectively consume the NaClO residing in the DX phase, unless the two phases are mixed to enhance cross-phase NaClO diffusion. This phenomenon allows us to design an oxidative extraction procedure as follows (Figure 2a): (1) start from the "oxidized"

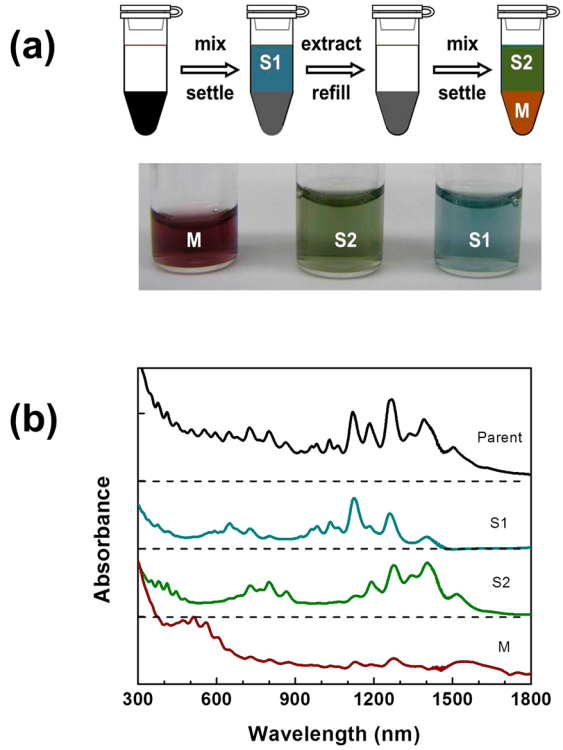

Figure 2. Fractionation of HiPco nanotubes by successive oxidative extraction. (a) Separation scheme and photographs of extracted fractions. (b) Optical absorption spectra of the parent HiPco material and fractions successively extracted from a PEG/DX ATP system with the aid of NaClO. "S1" and "S2" are two successive fractions extracted into the top PEG phase from the starting material, nanotubes remaining in the bottom DX phase are labeled "M" fraction.

regime by adding sufficient amount of NaClO; (2) shift the system to the "semi-oxidized" regime by repeatedly mixing the ATP system to gradually reduce the oxidative effect; (3) remove the top PEG phase and add fresh top phase to reconstitute the ATP system; (4) obtain more fractions by repeating steps 2 and 3 until all the nanotubes are extracted from the bottom to the top phase.

Figure 2 shows the result of a HiPco nanotube fractionation by such a successive extraction process using an ATP system composed of 6% PEG + 6% DX and 0.9% SC + 1% SDS. In the first step, 1 mM NaClO is added so that the system is in the "oxidized" regime with all the nanotubes residing in the bottom DX phase. Upon mixing and phase settling, smaller diameter/larger bandgap semiconducting tubes are extracted into the top PEG phase (fraction S1, panels a and b of Figure 2). The top phase is then removed and replaced with a fresh PEG phase. Upon further mixing and settling, a second fraction containing larger diameter/small bandgap semiconducting tubes is extracted (fraction S2, panels a and b of Figure 2). The change

DOI: 10.1021/nl504189p
Nano Lett. 2015, 15, 1642−1646

in bandgap from S1 to S2 is clearly indicated by the shift in the E11 and E22 absorption peaks toward longer wavelengths (Figure 2b). Remaining in the bottom DX phase are largely metallic tubes (fraction M, panels a and b of Figure 2), which are further fractionated by repeating the PEG phase extraction procedure.

Figure 3a shows the absorption spectra of four successively extracted metallic fractions M3 to M6 from the M fraction. We

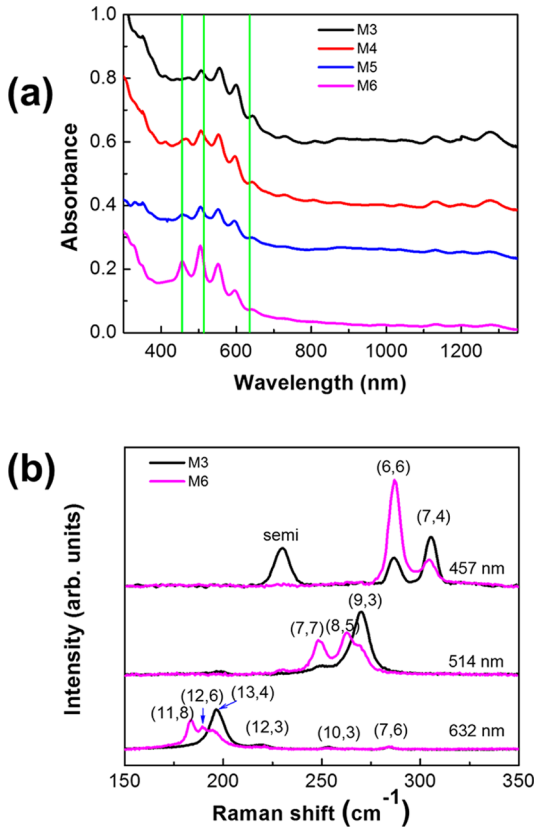

Figure 3. Spectroscopic characterization of fractions M3 to M6 successively extracted from the M fraction shown in Figure 2. (a) Absorbance spectra of M3 to M6. Vertical green lines indicate the wavelength positions of laser excitation used for the resonance Raman measurement. (b) RBM profiles of M3 (black traces) and M6 (magenta traces) measured at excitation wavelengths of 457, 514, and 632 nm, respectively. The spectra are normalized by integrated spectral area for easy comparison.

notice that the spectrum of M6 closely resembles that of the armchair-enriched fractions reported by Hároz et al.[16] To determine the difference in chirality distribution in the metallic fractions, we have measured the Raman radial breathing mode (RBM) profiles of M3 and M6 using three different excitation wavelengths. As shown in Figure 3b, metallic RBM peaks from M6 have higher peak intensities at lower Raman shifts. Chirality assignment further reveals that M6 has more RBM peak intensities from armchair or near-armchair tubes. This implies that M3 is enriched in smaller diameter and nonarmchair metallic tubes with higher $\cos(3\theta)/d^2$ values, whereas M6 is enriched in armchair or near-armchair and larger diameter tubes with lower $\cos(3\theta)/d^2$ values. In Supporting Information Figure S4, we show the bandgap distributions for the S1, S2, M3, and M6 fractions derived from spectral analysis. Taken together, our results demonstrate that the oxidative extraction process purifies SWCNTs in the order of large bandgap semiconducting tubes, small bandgap semiconducting tubes, semimetals of nonzero bandgap, and armchair tubes of zero-bandgap.

The oxidative extraction method has a number of distinct features. First, it is capable of fractionating metallic tubes by their vanishingly small bandgap, a feat that no other nanotube separation method has ever demonstrated. Second, we note that the oxidative extraction order for semiconducting tubes is opposite to that of the recently developed surfactant SDS/sodium deoxycholate (SDC)-based extraction, where a gradual increase (decrease) of the SDS (SDC) concentration leads to PEG phase extraction of larger diameter tubes first, followed by smaller diameter ones.[12,13] These two different mechanisms may be employed orthogonally to achieve better separation. Finally, in comparison with our previously reported SDS/SC based extraction process for metal/semiconductor separation,[14] the oxidative extraction works with a greatly expanded surfactant concentration range (0.4−1% for SC, 0.4−1% for SDS) and temperature range (15−30 °C), making the process much more reliable and robust. In light of the newly identified role played by redox, we suggest that our previously reported SDS/SC based extraction of metal/semiconductor SWCNTs is enabled by dissolved oxygen, the oxidation potential of which is sensitively dependent on factors such as temperature and pH, consequently making the process vulnerable to uncontrollable external changes.

Mechanistically, redox-induced change in nanotube partition in the ATP system is most likely the result of a surfactant coating layer reorganization triggered by electron transfer. Oxidation/reduction necessarily alters the electronic configuration or electron wave function of a nanotube, which in turn should alter the bonding between the nanotube and surfactant molecules. To accommodate changes in binding affinity, the surfactant layer must reorganize in composition and/or spatial arrangement, leading to a rescaling of solvation energies in the two phases.

The above analysis suggests that the redox effect should be a general phenomenon observable in other SWCNT separation processes. Indeed, a number of reported pH- and oxygen-dependent separation phenomena in density gradient ultracentrifugation (DGU)[17,18] and gel chromatography[19,20] are likely due to redox-triggered surfactant reorganization. To support this hypothesis, we have made direct observation of the redox effect on DGU and gel chromatography separations. In the case of DGU, Supporting Information Figure S2 shows that the buoyancy of SWCNTs, or the banding of SWCNT fractions are strongly modulated by redox potential. In the case of gel chromatography, Supporting Information Figure S3 shows that the elution pattern for semiconducting tubes is also dependent on redox condition, implying that the binding affinity of the surfactant-SWCNT complexes to the stationary phase polymer matrix is changed by surfactant reorganization.

We find that redox also affects SWCNT dispersion in organic solvents, further extending the role of redox in SWCNT separation. Polyfluorene and related polymer structures have been used for efficient extraction of semiconducting tubes in nonpolar solvents.[21] The mechanism of the selective extraction remains elusive despite many investigations. We have examined a few commercially available polyfluorene derivatives for the dispersion of various sources of SWCNTs. In all cases, we find that oxidizing condition enhances selective dispersion with a concomitant lowering of dispersion yield, whereas reducing condition does just the opposite. We suggest that nanotube

DOI: 10.1021/nl504189p
Nano Lett. 2015, 15, 1642−1646

oxidation (reduction) modifies the electronic structure and subsequently alters the binding affinity of the polymer to the nanotubes. This results in less stable (but more selective) dispersions under oxidative conditions and more stable (but less selective) dispersions under reducing conditions. Figure 4

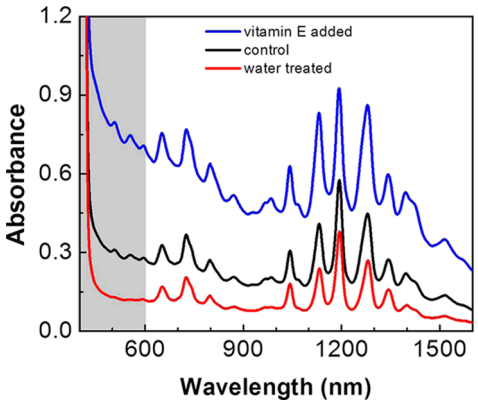

Figure 4. Absorption spectra of HiPco SWCNT dispersions in toluene made with same amount of PFO-bipy (1 mg/mL) and SWCNT (0.036 mg/mL) but under different redox conditions. Blue trace, dispersion made with 10 mM vitamin E added to the PFO-bipy/SWCNT mixture; black trace, control dispersion with no redox agent added; red trace, dispersion made from the control by adding 1/10 the sample volume of water, then bath sonication and centrifugation to remove the newly formed aggregates. Note that only a subset of semiconducting chirality species is present in the water-treated sample. This suggests that in addition to the redox effect, specific polymer/nanotube interactions also play a role in the selective dispersion.

shows an example of the redox effect on the dispersion of HiPco nanotubes by poly[(9,9-dioctylfluorenyl-2,7-diyl)-*alt*-co-(6,6′-{2,2′-bipyridine})] (PFO-bipy). Similar results are also obtained using the more common PFO polymer. A PFO-bipy/SWCNT mass ratio = 28 was used for the experiment. Consistent with a literature report,[22] selective dispersion of semiconducting tubes is compromised by the excess amount of PFO-bipy, as evident by the appearance of metallic SWCNT features in the (400 to 600) nm region (gray area in Figure 4) of the absorption spectrum (Figure 4, black trace). A mild oxidation treatment via the addition of 1/10 the sample volume of water followed by bath sonication induces preferential metallic tube aggregation, such that the remaining dispersion (Figure 4, red trace) is highly enriched in semiconducting tubes. Most likely this is caused by water-derived reactive oxygen species generated by sonication, which may directly or indirectly cause nanotube oxidation. In contrast, in the presence of 10 mM reducing agent vitamin E, PFO-bipy disperses nearly all chiral species nonselectively (Figure 4, blue trace). We also find that the reduced (vitamin E treated) SWCNTs can be oxidized by water treatment, implying reversibility. However, the oxidized (water-treated) SWCNTs are not readily reduced, due primarily to the difficulty in complete removal of water from toluene. Our findings show that solubility of polymer-wrapped SWCNTs in organic solvents is strongly dependent on the redox status of the solvent environment. Ambient redox condition fortuitously enables certain polymers to selectively extract semiconducting tubes under a narrow polymer/SWCNT mass ratio. Our findings also suggest that controlled oxidation may be used to enhance the semiconducting tube selectivity for those polymers[23] that lack the capability under ambient conditions.

In summary, we have shown that redox strongly affects the structure of the surfactant coating layer and consequently nanotube separation outcome. Ambient redox condition set by the dissolved oxygen and uncontrolled pH (in aqueous systems) is conducive to a number of SWCNT separation processes, but may not necessarily represent the optimum conditions. Revelation of the hidden role played by redox highlights the importance of regulating this parameter for more reproducible separation outcome and points to the possibility of redox tuning of coating layer structures to enhance separation resolution. Going beyond nanotube separation, it is foreseeable that redox triggered surfactant reorganization may also affect other colloidal behavior of SWCNTs.

■ ASSOCIATED CONTENT

Supporting Information

Figures S1, S2, S3, and S4 and experimental details. This material is available free of charge via the Internet at http://pubs.acs.org.

■ AUTHOR INFORMATION

Corresponding Authors

*E-mail: (M.Z.) ming.zheng@nist.gov.
*E-mail: (C.Z.) chongwuz@usc.edu.

Notes

The authors declare no competing financial interest.

■ ACKNOWLEDGMENTS

This work is support in part by a grant from AFOSR. J.K.S. acknowledges a National Research Council postdoctoral fellowship.

■ REFERENCES

(1) Iijima, S.; Ichihashi, T. Single-shell carbon nanotubes of 1-nm diameter. *Nature* **1993**, *363* (6430), 603−605.
(2) Saito, R.; Fujita, M.; Dresselhaus, G.; Dresselhaus, M. S. Electronic structure of chiral graphene tubules. *Appl. Phys. Lett.* **1992**, *60* (18), 2204−2206.
(3) Mistry, K. S.; Larsen, B. A.; Blackburn, J. L. High-Yield Dispersions of Large-Diameter Semiconducting Single-Walled Carbon Nanotubes with Tunable Narrow Chirality Distributions. *ACS Nano* **2013**, *7* (3), 2231−9.
(4) Hamada, N.; Sawada, S.-i.; Oshiyama, A. New one-dimensional conductors: Graphitic microtubules. *Phys. Rev. Lett.* **1992**, *68* (10), 1579−1581.
(5) Kane, C. L.; Mele, E. J. Size, Shape, and Low Energy Electronic Structure of Carbon Nanotubes. *Phys. Rev. Lett.* **1997**, *78* (10), 1932−1935.
(6) Ouyang, M.; Huang, J.-L.; Cheung, C. L.; Lieber, C. M. Energy Gaps in "Metallic" Single-Walled Carbon Nanotubes. *Science* **2001**, *292* (5517), 702−705.
(7) Odom, T. W.; Huang, J.-L.; Kim, P.; Lieber, C. M. Atomic structure and electronic properties of single-walled carbon nanotubes. *Nature* **1998**, *391* (6662), 62−64.
(8) Strano, M. S.; Huffman, C. B.; Moore, V. C.; O'Connell, M. J.; Haroz, E. H.; Hubbard, J.; Miller, M.; Rialon, K.; Kittrell, C.; Ramesh, S.; Hauge, R. H.; Smalley, R. E. Reversible, Band-Gap-Selective Protonation of Single-Walled Carbon Nanotubes in Solution. *J. Phys. Chem. B* **2003**, *107* (29), 6979−6985.
(9) Zheng, M.; Diner, B. A. Solution Redox Chemistry of Carbon Nanotubes. *J. Am. Chem. Soc.* **2004**, *126* (47), 15490−15494.
(10) Hirana, Y.; Juhasz, G.; Miyauchi, Y.; Mouri, S.; Matsuda, K.; Nakashima, N., Empirical Prediction of Electronic Potentials of Single-

DOI: 10.1021/nl504189p
Nano Lett. 2015, 15, 1642−1646

Walled Carbon Nanotubes With a Specific Chirality (n,m). *Sci. Rep.* **2013**, *3*.
(11) Schäfer, S.; Cogan, N. M. B.; Krauss, T. D. Spectroscopic Investigation of Electrochemically Charged Individual (6,5) Single-Walled Carbon Nanotubes. *Nano Lett.* **2014**, *14* (6), 3138−3144.
(12) Zhang, M.; Khripin, C. Y.; Fagan, J. A.; McPhie, P.; Ito, Y.; Zheng, M. Single-Step Total Fractionation of Single-Wall Carbon Nanotubes by Countercurrent Chromatography. *Anal. Chem.* **2014**, *86* (8), 3980−3984.
(13) Fagan, J. A.; Khripin, C. Y.; Silvera Batista, C. A.; Simpson, J. R.; Hároz, E. H.; Hight Walker, A. R.; Zheng, M. Isolation of Specific Small-Diameter Single-Wall Carbon Nanotube Species via Aqueous Two-Phase Extraction. *Adv. Mater.* **2014**, *26* (18), 2800−2804.
(14) Khripin, C. Y.; Fagan, J. A.; Zheng, M. Spontaneous Partition of Carbon Nanotubes in Polymer-Modified Aqueous Phases. *J. Am. Chem. Soc.* **2013**, *135* (18), 6822−6825.
(15) Luo, C.; Zhang, Y.; Zeng, X.; Zeng, Y.; Wang, Y. The role of poly(ethylene glycol) in the formation of silver nanoparticles. *J. Colloid Interface Sci.* **2005**, *288*, 444−448.
(16) Hároz, E. H.; Rice, W. D.; Lu, B. Y.; Ghosh, S.; Hauge, R. H.; Weisman, R. B.; Doorn, S. K.; Kono, J. Enrichment of Armchair Carbon Nanotubes via Density Gradient Ultracentrifugation: Raman Spectroscopy Evidence. *ACS Nano* **2010**, *4* (4), 1955−1962.
(17) Homenick, C. M.; Rousina-Webb, A.; Cheng, F.; Jakubinek, M. B.; Malenfant, P. R. L.; Simard, B. High-Yield, Single-Step Separation of Metallic and Semiconducting SWCNTs Using Block Copolymers at Low Temperatures. *J. Phys. Chem. C* **2014**, *118* (29), 16156−16164.
(18) Antaris, A. L.; Seo, J.-W. T.; Brock, R. E.; Herriman, J. E.; Born, M. J.; Green, A. A.; Hersam, M. C. Probing and Tailoring pH-Dependent Interactions between Block Copolymers and Single-Walled Carbon Nanotubes for Density Gradient Sorting. *J. Phys. Chem. C* **2012**, *116* (37), 20103−20108.
(19) Hirano, A.; Tanaka, T.; Urabe, Y.; Kataura, H. pH- and Solute-Dependent Adsorption of Single-Wall Carbon Nanotubes onto Hydrogels: Mechanistic Insights into the Metal/Semiconductor Separation. *ACS Nano* **2013**, *7* (11), 10285−10295.
(20) Flavel, B. S.; Kappes, M. M.; Krupke, R.; Hennrich, F. Separation of Single-Walled Carbon Nanotubes by 1-Dodecanol-Mediated Size-Exclusion Chromatography. *ACS Nano* **2013**, *7* (4), 3557−3564.
(21) Nish, A.; Hwang, J.-Y.; Doig, J.; Nicholas, R. J. Highly selective dispersion of single-walled carbon nanotubes using aromatic polymers. *Nat. Nanotechnol.* **2007**, *2* (10), 640−646.
(22) Mistry, K. S.; Larsen, B. A.; Blackburn, J. L. High-Yield Dispersions of Large-Diameter Semiconducting Single-Walled Carbon Nanotubes with Tunable Narrow Chirality Distributions. *ACS Nano* **2013**, *7* (3), 2231−2239.
(23) Rice, N. A.; Adronov, A. Supramolecular Interactions of High Molecular Weight Poly(2,7-carbazole)s with Single-Walled Carbon Nanotubes. *Macromolecules* **2013**, *46* (10), 3850−3860.

DOI: 10.1021/nl504189p
Nano Lett. 2015, 15, 1642−1646